International Journal of Biological Macromolecules 362 (2026) 152050

Contents lists available at ScienceDirect

International Journal of Biological Macromolecules

journal homepage: www.elsevier.com/locate/ijbiomac

Time meets protein corona: the Vroman effect dictates macrophage recognition of PEGylated nanoparticles

Alejandro Cortés-Bazo [a,b,1], José C. García-Perdiguero [a,b,1], Natividad Gómez-Cerezo [a,b,*], Miguel Gisbert-Garzarán [a,b,*], María Vallet-Regí [a,b,*]

[a] Departamento de Química en Ciencias Farmacéuticas, Universidad Complutense de Madrid, Spain
[b] Instituto de Investigación Sanitaria Hospital, 12 de Octubre i+12, Plaza Ramón y Cajal s/n, Madrid, 28040, Spain

ARTICLE INFO

Keywords:
Protein Corona
Vroman Effect
Time-Evolution
Nanoparticles
Drug Delivery
Clearance
Macrophages

ABSTRACT

The phenomenon of the protein corona is a major contributor to the limited bench-to-bedside translation of nanomedicines, as it confers a new biological identity that can lead to rapid bloodstream clearance. The composition of the protein corona is dynamic and varies over time. This so-called Vroman effect implies that nanoparticles (NPs) should display a time-dependent biological identity that would modulate how they interact with the living environment as time evolves. Incorporating polyethylene glycol (PEG) into nanoformulations is the gold-standard for minimizing this rapid recognition by the immune system. Nonetheless, whether the protein corona and, consequently, the biological identity imparted by this stealth polymer are immutable over time remain unexplored. Here, we provide a facile assay to evaluate how the Vroman effect dictates macrophage recognition of NPs upon incubation with plasma. For that purpose, we have engineered two types of PEGylated mesoporous silica nanoparticles that have been subjected to short-term (5 min) or long-term (1 h) incubation with human plasma to allow for protein corona formation. The physicochemical characterization has demonstrated appreciable changes according to the incubation time (*e.g.*, mean size, amount of protein adsorbed…). The protein coronas have been fully analyzed by means of proteomics, validating the existence of an underlying Vroman effect. The key finding and novelty of our work is that flow cytometry experiments of time-dependent protein coronas suggest the existence of a transient, undesired protein corona that enhances immune recognition before evolving into a less immunogenic state, regardless of the PEGylation degree. Altogether, these findings open the door to more exhaustive analyses of nanomedicines and could contribute to the rational design of *in vivo* experimentation.

1. Introduction

The insufficient understanding of how nanoparticles (NPs) interact with biological components is a major contributor to the limited number of clinically available nanomedicines. In this sense, following bloodstream administration, blood proteins rapidly form a *protein corona* onto the NPs surface that endows them with a novel biological identity [1]. The composition of such protein layer is governed by several parameters, including NP surface chemistry, size, shape or charge or calcium content, among others [2,3]. Hence, acquiring a *bad* corona can trigger immune recognition and accelerate bloodstream clearance, thereby preventing effective drug delivery [4]. The formation of the protein corona is a dynamic process governed by the Vroman effect. This phenomenon establishes that proteins adsorb onto a surface in a time-dependent manner: proteins with higher diffusion rates and concentrations adsorb first to be gradually replaced by those with the highest affinity towards the surface [5]. In consequence, if the protein composition varies over time, so should the biological identity and how such NPs interact with the immune system.

The field of protein corona is still at an early stage and increased understanding of this phenomenon is expected to arise in the near future. In this sense, recent development of data science, machine learning and nanoinformatics is expected to help predict nanomaterial behavior and corona formation in biological fluids [6,7]. In this regard, such powerful tools depend on generating robust sets of empirical data to supply the high-quality datasets necessary to train future artificial

* Corresponding authors at: Departamento de Química en Ciencias Farmacéuticas, Universidad Complutense de Madrid, Spain
E-mail addresses: magome21@ucm.es (N. Gómez-Cerezo), migisber@ucm.es (M. Gisbert-Garzarán), vallet@ucm.es (M. Vallet-Regí).
[1] Both authors contributed equally

https://doi.org/10.1016/j.ijbiomac.2026.152050
Received 19 January 2026; Received in revised form 13 April 2026; Accepted 15 April 2026
Available online 21 April 2026
0141-8130/© 2026 The Author(s). Published by Elsevier B.V. This is an open access article under the CC BY license (http://creativecommons.org/licenses/by/4.0/).

intelligence models. This will help to understand protein-NP interactions, which are of major importance to comprehend biological interactions [2]. In this context, recent research has shown that the binding ratio of targeted NPs to cell receptors highly depends on serum proteins-NP interactions. Hence, optimizing NP parameters so as to show higher affinity towards cell receptors than towards serum proteins may help to improve NP design [8].

Polyethylene glycol (PEG) has traditionally been shown to confer stealth properties to NPs, which translates into extended circulation time. Researchers have paid attention to how multiple parameters influence this camouflage performance, including PEG molecular weight, surface density or spatial conformation [9,10]. Even though several research articles evaluate the protein corona of nanomaterials at a fixed time point, only a small fraction has attempted to unravel the underlying Vroman effect. Because of the high complexity of human serum, precise analysis of the kinetics and physicochemical features of the corona formation on NPs over time remains challenging and limited to mixtures containing few proteins [11,12]. Nonetheless, protein determination by mass spectrometry allows the time-dependent elucidation of coronas originating from complex mixtures along with its correlation with the NP biological performance [13–18]. Such studies have shown the existence of time-dependent protein coronas depending on the surface chemistry (*e.g.*, COOH or NH_2 groups), *i.e.*, the Vroman effect. However, how the PEG-induced protein corona composition evolves over time remains missing.

The rationale behind this piece of research was answering the following questions: (i) is the PEG-induced biological identity fixed and consistent over time? (ii) is the Vroman effect relevant enough to govern the overall biological identity? (iii) is the Vroman effect relevant enough to impair the PEG-induced stealth properties? To the best of our knowledge, this is the first time that this phenomenon and how it may trigger immune recognition has been reported. We have employed mesoporous silica nanoparticles (MSNs) as model platform to shed light on such questions (Scheme 1). MSNs have been extensively employed in the development of nanoformulations for controlled drug release. In addition to the remarkable textural properties that allow the loading of high amounts of therapeutics, MSNs are easy to synthesize and present a surface full of silanol groups that allow the straightforward functionalization of the surface with further functionalities (*e.g.*, PEG). These NPs are robust and provide a reliable platform to assess the phenomenon of the protein corona [19]. Overall, two PEG grafting densities (10% *w*/w and 20% w/w *vs.* MSNs) and three incubation conditions with human plasma have been employed, namely: no plasma incubation ($t = 0$), short-term incubation (5 min), and long-term incubation (1 h). In this sense, it has been shown that the first 5 min after bloodstream administration are crucial for the fate of the NPs, observing up to 90% of clearance within such 5 min if the immune system detects the NPs. Conversely, prolonged blood circulation is expected if the NPs overcome the initial stage [20]. Each of the above-mentioned incubation conditions has been physicochemically characterized and the different protein coronas have been thoroughly analyzed by means of proteomics. Finally, the distinct biological NP identities have been assessed in macrophage-like THP-1 human cells to elucidate if temporal factors modulate macrophage recognition, helping to understand whether the Vroman effect plays a relevant role in nanomedicine.

2. Materials and methods

The following compounds were purchased from Sigma-Aldrich Inc.: tetraethyl orthosilicate (TEOS), hexadecyltrimethylammonium bromide (CTAB), sodium hydroxide (NaOH), 3-aminopropyl triethoxysilane (APTES), fluorescein isothiocyanate isomer I (FITC), ammonium nitrate, (3-triethoxysilyl)propyl succinic anhydride (SATES), methoxypolyethylene glycol amino (5000 g/mol) (mPEG5k-NH2).

2.1. Synthesis of PEGylated MSNs (5k10 & 5k20)

MSNs were synthesized following our previously reported method with minor modifications [21]. Briefly, H_2O (480 mL), NaOH (3.5 mL, 2 M) and CTAB (1 g) were placed in a 1-L round bottom flask. The mixture was heated at 80 °C for 30 min. Then, TEOS (5 mL) was added dropwise (5 mL/min) and the whole reaction mixture was stirred at 80 °C for further 2 h. Afterwards, the reaction was cooled down in an ice bath, centrifuged, and washed twice with ethanol (50% in water). The organic template was then removed using an ethanolic solution (95% in water) containing ammonium nitrate (10 mg/mL). For that purpose, the NPs were dispersed in 350 mL of such solution and refluxed overnight. After that, they were centrifuged and washed once with ethanol and water. Then, the NPs were dispersed again in 350 mL of that solution and refluxed for 4 h. Finally, the MSNs were centrifuged, washed twice with ethanol and water and dried at 70 °C. For the cellular experiments, FITC-labelled NPs were employed. For that purpose, APTES (2.2 μL) was reacted with FITC (1 mg) in ethanol (40 μL) for 2 h. Then, the mixture was carefully mixed with TEOS, and the above-described protocol was

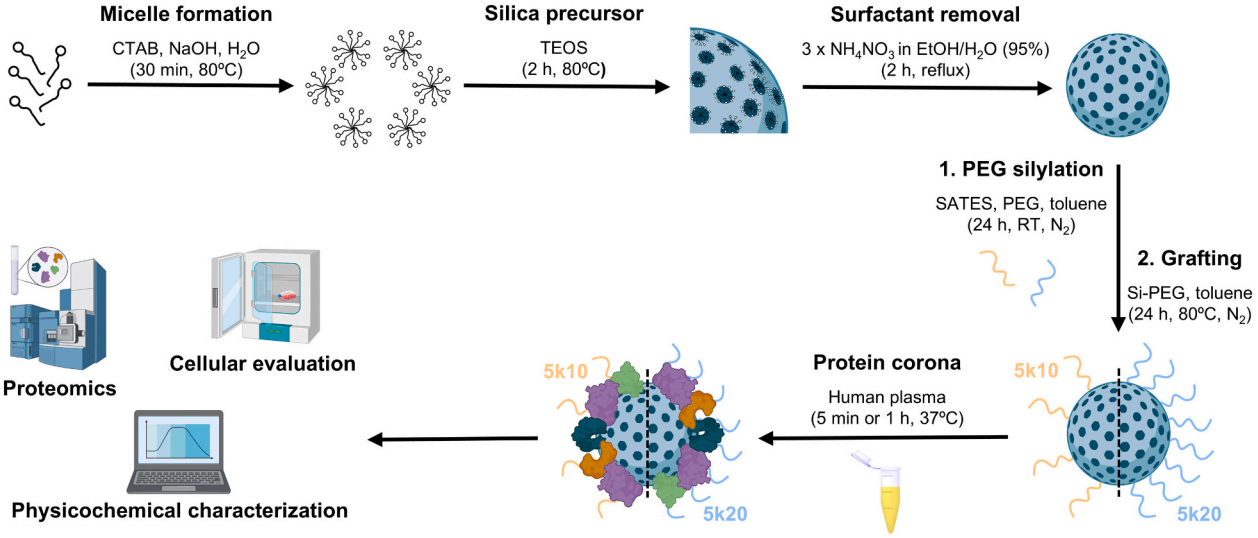

Scheme 1. Schematic workflow of this research. MSNs were synthesized following a *sol-gel* methodology, and PEG was grafted using an alkoxysilane as linker. Protein coronas were generated at different time points, and the outcome was analyzed using physicochemical techniques, flow cytometry and proteomics.

carried out again.

The as-synthesized NPs were functionalized with mPEG5k-NH_2 using two grafting densities, namely 10% or 20% (*w*/w *vs.* MSNs). The PEGylated NPs were denoted as 5k10 and 5k20. The synthesis of 5k10 is shown as a representative example. All reactions were carried out in N_2-purged containers. First, mPEG5k-NH2 (7.5 mg, 1 eq) was dissolved in anhydrous toluene (1.5 mL). Then, SATES (0.68 mg, 1.5 eq) was dissolved in anhydrous toluene (0.5 mL) and further added to the PEG solution. The mixture was allowed to react overnight at 35 °C. MSNs (75 mg) were then dried under vacuum (1 h, 100 °C) to remove water traces and subsequently dispersed in anhydrous toluene (15 mL). Afterwards, the silylated PEG was added dropwise and the whole reaction mixture was stirred overnight at 80 °C. Finally, the PEG-coated NPs were centrifuged, washed three times with ethanol and dried in an oven at 70 °C.

The above-synthesized nanomaterials were physicochemically characterized by means of transmission electron microscopy (TEM microscopy), dynamic light scattering (DLS), Fourier-transformed infrared spectroscopy (FTIR spectroscopy) and thermogravimetric analysis.

2.2. Protein corona

The NPs were incubated with human plasma (Sigma-Aldrich) to generate protein coronas following our previous methodology [22]. For that purpose, the corresponding material (0.5 mg) was dispersed in 300 μL of distilled water. Then, 75 μL of human plasma were added and the samples were placed in a thermoshaker (37 °C, 600 rpm) for either 5 min or 1 h. After each time point, the whole volume was loaded onto a sucrose cushion (0.9 mL, 0.7 M), centrifuged and washed twice with distilled water (1.2 mL). Finally, the pellets were stored at −20 °C for further analysis. Samples were denoted as 5k10–5 min, 5k10-1 h, 5k20-5 min and 5k20-1 h.

A Micro BCA™ Protein Assay Kit (Thermo Fisher) was employed to quantify the amount of proteins adsorbed onto each NP. Briefly, each pellet was dispersed in 500 μL of PBS. Then, 30 μL of the previous dispersion were diluted with 120 μL of PBS and placed in a 96-well plate. After that, 150 μL of working reagent were added to each well and the assay was carried out and measured following the manufacturer's instructions (absorbance, 562 nm). NPs without a protein corona were used as controls to exclude potential interferences.

The identity of the adsorbed proteins was unveiled using the proteomics facility at the Spanish National Center for Biotechnology. The samples were measured in an Orbitrap Exploris 240 spectrometer and the raw data were analyzed using the Proteome Discoverer Software. The experimental protocol was carried out as reported in a previous study [23]. Proteins are expressed throughout the text according to the corresponding gene. The reader is referred to the Supporting Information for a complete list of protein names.

2.3. Cellular experiments

Cells were incubated in a 5% CO_2 incubator at 37 °C for all the experiments. THP-1 human monocytes were cultured in RPMI-1640 + Glutamax supplemented medium (Gibco, Waltham, MA, USA) containing 10% (*v*/v) heat-inactivated fetal bovine serum (FBS, Gibco, BRL, UK) and 1% penicillin/streptomycin mixed solution (Nacalai Tesque Inc., Kyoto, Japan). Prior to the experiments, the THP-1 cells were differentiated into M0 macrophages. For that purpose, cells were treated with PMA (100 ng/mL) phorbol myristate acetate (PMA) (Sigma, Munich, Germany) for 24 h, followed by a 24-h incubation with fresh medium.

The protein corona-coated NPs were freshly prepared right after incubation with cells (5k-5 min; 5k-1 h). Following corona formation, each group was redispersed in distilled water and diluted in FBS-free culture medium to a concentration of 100 μg/mL. NPs without a previously formed protein corona were included as control to assess the nanomaterial itself (5k-0 min). Similarly, NPs directly placed in FBS-containing culture medium (5k-FBS), *i.e.*, standard condition to analyze nanomaterials in cell cultures, were also included as control.

2.3.1. Cell viability

The Alamar Blue (AB) assay was carried out to assess if the different pre-formed coronas affected the viability of the cells. For that purpose, THP-1 cells were seeded at a density of $2{\cdot}10^4$ cells per well in 96-well plates. Then, the corresponding NPs (5k-0 min; 5k-5 min; 5k-1 h) were incubated with the cells at a concentration of 100 μg/mL for 3 h to trigger cellular uptake. After 24 and 48 h, 100 μL of AB solution (5% [*v*/v] solution of AB dye, AbD Serotec, Oxford, UK) in RPMI) were added to each well. The solution was left to react for 3 h and then, each well was transferred to a 96-well plate for fluorescence quantification (λexc = 540 nm, λem = 595 nm) in a FLUOstar Omega (BMG LABTECH).

2.3.2. Cellular uptake by flow cytometry

THP-1 cells were seeded at a density of $3{\cdot}10^5$ per well in 6-well plates. The different conditions (5k-FBS; 5k-0 min; 5k-5 min; 5k-1 h) were added at a concentration of 100 μg/mL and incubated for 3 h. Except for 5k-FBS, all conditions were incubated in serum-free culture medium to avoid interference of FBS proteins with the preformed corona. Then, the media was removed, and cells were washed twice with PBS to remove non-internalized NPs. Cells were detached with trypsin, which was further inactivated with FBS-containing RPMI. Finally, cells were redispersed in PBS and measured in an Attune NxT Acoustic Focusing Cytometer (Invitrogen, Thermo Fisher Scientific). Internalization was determined based on the mean fluorescence intensity of the samples (at least $2{\cdot}10^4$ cells per condition). Forward scatter (FSC) and side scatter (SSC) were also analyzed in the flow cytometer.

3. Results and discussion

3.1. Physicochemical characterization of the time-dependent protein corona

MSNs were synthesized following a modified Stöber method, using CTAB as cationic surfactant and TEOS as silica precursor. The NPs were further PEGylated using an amine-reactive alkoxysilane as linker, yielding 5k10 and 5k20, *i.e.*, MSNs functionalized with PEG (5000 g/mol) at either 10 or 20% *w*/w. It is generally accepted the existence of a molecular weight threshold for PEG. In this sense, PEG below 2 kDa is ineffective in preventing protein adsorption on NPs. In addition, it seems that increasing the molecular weight to 5 kDa would be beneficial for avoiding immune cell uptake than the 2 kDA, which would be ascribed to the different spatial conformations that can adopt [9,24]. The experimental degree of PEGylation was determined by thermogravimetric analysis (14.53% for 5k10; 21.76% for 5k20, Fig. S0). Both NPs were visually inspected by TEM micrography, demonstrating the formation of porous nanocarriers with size in the range 150–200 nm (Fig. 1, left). The proper formation of the silica backbone along with the successful grafting of the polymer was verified by the appearance of the typical vibration bands of mesoporous silica materials and those ascribed to C—H bonds from the PEG (Fig. S1A—B).

The protein corona formed upon incubation with plasma was visualized *via* TEM, revealing the presence of organic matter around the NPs (Fig. 1, middle and left). The amount of adsorbed proteins was quantified using a micro BCA assay (Fig. 2A). No relevant differences were found between groups after the 5-min incubation (hereafter termed 5k-5 min when referring to both groups), whereas a marked reduction was observed in both cases after 1 h (hereafter termed 5k-1 h when referring to both groups). This trend suggests the dynamic nature of the protein corona, at least from the abundance point of view. In this sense, the organic coating visualized around 5k-5 min seemed to be more prominent than that around 5k-1 h (Fig. 1, middle and left), which would be in line with the previous micro BCA assay. The presence of this protein layer was further analyzed by DLS (Fig. 2B). As expected, the mean size

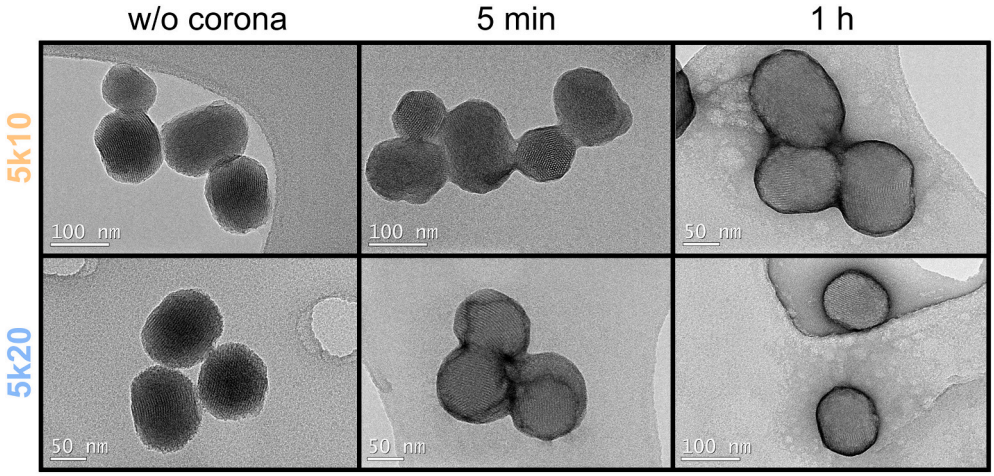

Fig. 1. TEM micrographs of 5k10 and 5k20 without corona (left), after a 5-min incubation in plasma (middle), and after a 1-h incubation in plasma (right). Samples undergoing plasma incubation were stained with uranyl acetate for organic matter visualization.

of all NPs increased upon incubation with human plasma, regardless of the incubation time. Interestingly, the increment *vs.* the corona-free NPs was much higher for 5k20 (5 min: 44%, 1 h: 35%) than for 5k10 (5 min: 31%, 1 h: 25%). This observation might be related to the presence of different spatial conformations as PEG density increased [25]. Finally, the formation of the protein corona was qualitatively unveiled *via* FTIR spectroscopy thanks to the appearance of vibration bands ascribed to the peptide bonds found in proteins (Fig. S1C—B).

3.2. Elucidation of the protein coronas by mass spectrometry

The detailed composition of the protein coronas was thoroughly studied by mass spectrometry. Initially, the proteins were classified according to biological processes of the blood system (Fig. 2C). Overall, the PEG density dictated the composition of the coronas, observing clear differences between 5k10 and 5k20. In this sense, 5k10 preferentially adsorbed proteins related to coagulation processes at both time points, whereas a balance between coagulation proteins and immunoglobulins was mainly observed for 5k20. Of note, a closer look at the numerical values revealed abundance changes over time for all biological processes of the blood, supporting the existence of an underlying Vroman effect (Table S1).

In absolute terms, all groups recruited similar number of proteins for each biological process, regardless of the incubation time. Nonetheless, this was unrelated to the abundance of such category in the sample. In this sense, less than 8% of coagulation proteins translated into them being the most abundant category in all cases (Fig. S2, Tables S1 and S4). This supports the widely held view that protein affinity towards the NPs surface plays a key role in the protein corona formation. The proteins were further analyzed for similarities using a Venn diagram (Fig. 2D), revealing (i) that most of the proteins were common among groups and (ii) the existence of unique proteins. This suggests that the Vroman effect understood in the sense of dynamic variation of protein identity is measurable and endows the NPs with a time-dependent biological identity. In agreement with the high degree of protein similarity, the analyses of both molecular weight (Fig. 2E) and isoelectric point (Fig. 2F) were rather similar among groups, regardless of the incubation time. In this sense, *ca.* 70% of the identified proteins had a molecular weight of 60 kDa or less, and most of them presented an isoelectric point in the range 6–9.

The analysis was sequentially restricted to the 100 (top 100) and 20 (top 20) most abundant proteins in each sample to gain insight into the predominant nature of the protein coronas. Even though the overall abundance of each category did not vary that much as the restriction increased (Fig. S2A), the number of proteins within each category dramatically changed, showing an enrichment in those that were most abundant, *i.e.*, coagulation, immunoglobulins and complement proteins (Fig. S2B). Similarly, sequential restriction to the 20 most abundant proteins altered the initially observed molecular weight and isoelectric point patterns (Fig. S3).

Each category shown in Fig. 2C was further split into the individual proteins to unveil the most relevant proteins within each biological process (Fig. 3A-F, top 100). Except for 5k10-1 h, FGA was the most abundant coagulation protein. IGHG1 clearly dominated the adsorbed immunoglobulins. All samples presented an increasing amount of C4A, being especially dominant in 5k20. Similarly, APOE constituted the most abundant lipoprotein in all cases. ITIH4 was the predominant acute phase protein, observing a drastic reduction at 1 h in all cases. Finally, GSN dominated the proteins ascribed to other processes, showing more abundance than all acute-phase and lipoproteins together. Fig. S4 provides further insights into the composition of the top 20 proteins. In addition to remaining the most abundant group, coagulation proteins became the most numerous (7/20 *vs.* 13/100). APOE was the only lipoprotein found in all cases except for 5k10–5 min, which also presented APOA1, and ITIH4 was the only acute phase protein among the top 20 proteins (excluding 5k20-1 h). GSN was the most abundant protein ascribed to other biological processes, and both nanomaterials were enriched in VTN at 1 h.

The existence of a Vroman effect understood in the sense of dynamic variation of protein abundance is visually supported in Fig. 3G. Regarding 5k10, the most abundant proteins at both time points were FGA (top 1 in 5k10–5 min), FGB (top 1 in 5k10-1 h), FGG and IGHG1, which together account for 76% (5k10–5 min) and 73.5% (5k10-1 h) of abundance, respectively. Compared to the 5-min plasma incubation, abundance values changed for all proteins in the list, being especially notorious for C4A (+36%), PLG (+56%), ITIH4 (−56%), APOE (+75%), and HRG (+150%). With regard to 5k20, IGHG1 led the list at both time points with minor changes, whereas the rest underwent variations in all cases. Outstanding examples are FGA (−43%), FGB (−42%), FGG (−45%), C4A (+82%), PLG (+72%), HRG (+125%), and APOE (+92%). Hence, considering all the data shown here, it can be undoubtedly concluded that the Vroman effect of PEGylated NPs does exist and manifest itself as either appearance/disappearance of proteins and/or as variation in abundance over time.

3.3. Influence of the Vroman effect on the biological identity of PEGylated NPs

Having confirmed the dynamic nature of the protein coronas, *i.e.*, the Vroman effect, our next goal was to evaluate whether those distinct

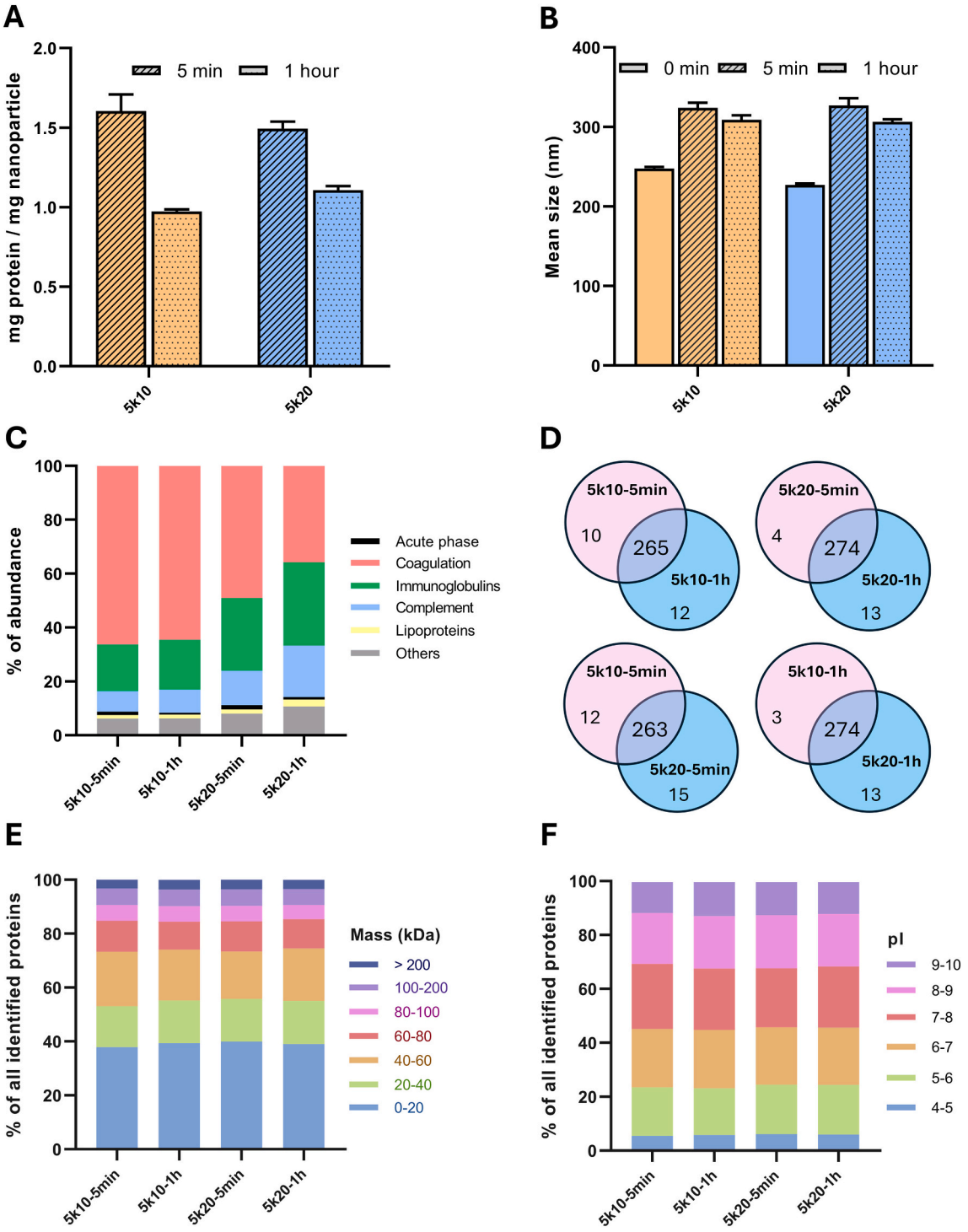

Fig. 2. Protein corona analysis (I). (A) Protein quantification by micro BCA assay. (B) Colloidal stability of the different NPs in the absence or presence of a protein corona. (C) Adsorbed proteins classified according to biological processes of the blood in terms of percentage of abundance within each category. (D) Venn diagram showing similarities and exclusive proteins for each sample. (E) Adsorbed proteins classified according to their molecular weight. (F) Adsorbed proteins classified according to their isoelectric point.

coronas might modulate how cells from the immune system would *see* the PEGylated NPs. Despite varying the incubation time led to different coronas (Section 2.2), the biocompatibility of the PEGylated NPs was unaffected by the underlying Vroman effect (Fig. S5A). Similarly, FSC and SSC remained almost constant after cellular uptake, demonstrating that NPs internalization did not produce cell retraction or increased significantly the cell complexity, regardless of the biological identity (Fig. S5B-E).

Fig. 4A depicts the workflow for analyzing macrophage recognition. In addition to the corresponding corona-coated NPs, those without corona (FBS-free medium, 5k-0 min) or those directly placed in cell culture medium (10% FBS, 5k-FBS) were included as controls. NPs were incubated with macrophages for either 45 min (Fig. 4B) or 180 min (Fig. 4C) to find out the uptake kinetics. In this sense, all groups but 5k10-FBS showed increased uptake after 180 min of experiment, which might suggest the existence of exocytosis events in the latter (Fig. S5F-

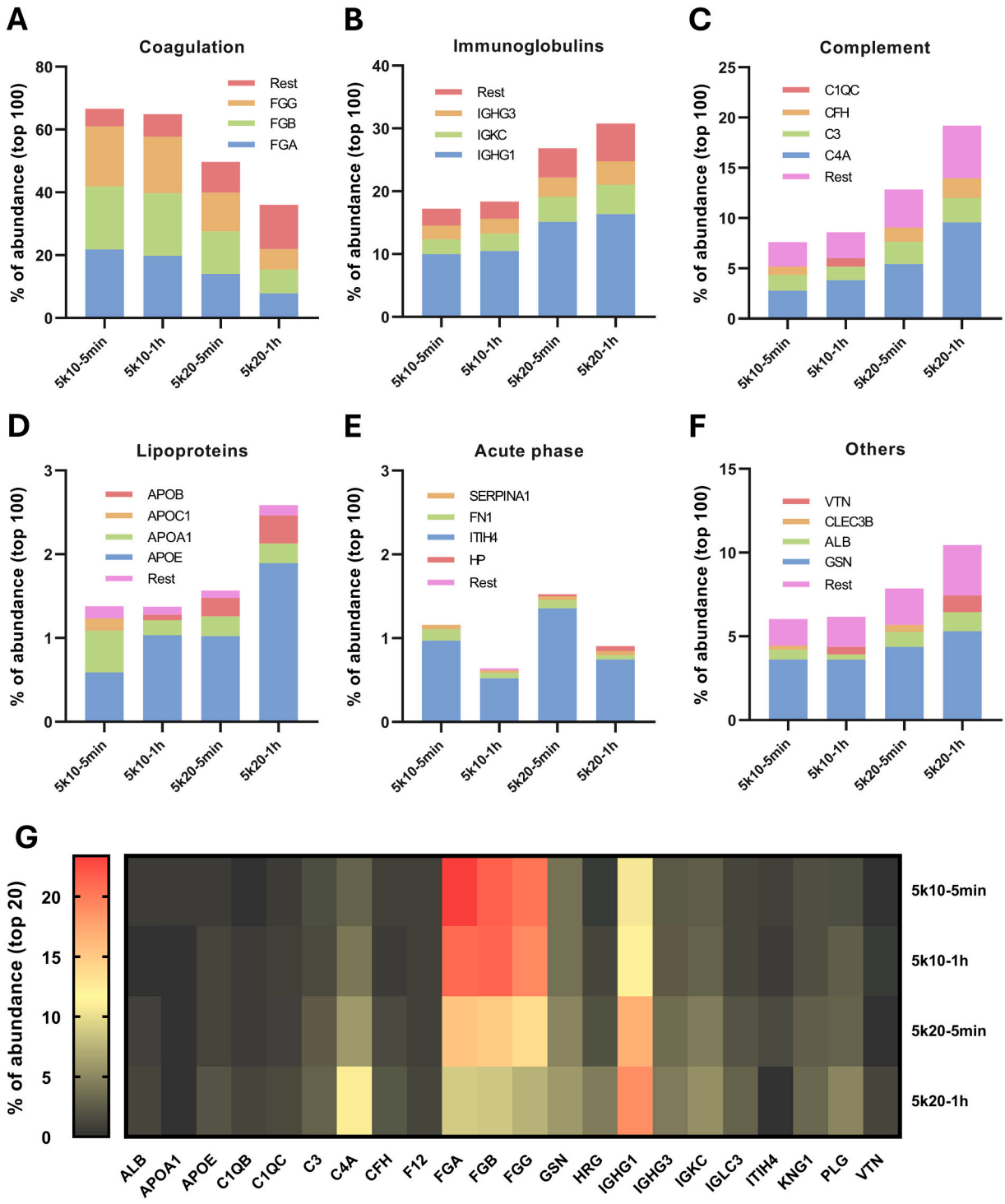

Fig. 3. Protein corona analysis (II). Detailed analysis of the most representative proteins (top 100) classified according to biological processes of the blood. From (A) to (F): Coagulation, immunoglobulins, complement, lipoproteins, acute phase, and others. (G) Heatmap displaying the abundance changes among the top 20 most abundant proteins for each sample.

G). It is worth mentioning that both FBS conditions clearly dominated the uptake after the 45 min-incubation and almost did after the 180 min one (Fig. 4B-C). This highlights the need to use human proteins (*e.g.*, human plasma) to analyze potential clearance of NPs by immune cells. Our results support the existence of interspecies effect on this phenomenon, which might lead to misinterpretation of results [26].

A seminal research article in the field of protein corona demonstrated that a protein corona is needed for the stealth effect of PEGylated NPs. The authors observed increased phagocytosis of those NPs lacking a protein corona compared to those that had been incubated for 1 h in human plasma [27]. Our data agrees with these groundbreaking results (Fig. 4B-C, 0 min *vs.* 1 h). Strikingly, the short-term condition led to rather different trends, showing increased phagocytosis than both the non-coated NPs (Fig. 4C, 5 min *vs.* 0 min) and those incubated for 1 h in human plasma (Fig. 4B-C, 5 min *vs.* 1 h). So far, the scientific consensus has been that it is the specific proteins recruited by PEG that impart stealth properties rather than the polymer itself [27]. Here, the results found for the short-term incubation seem to oppose such paradigm. This

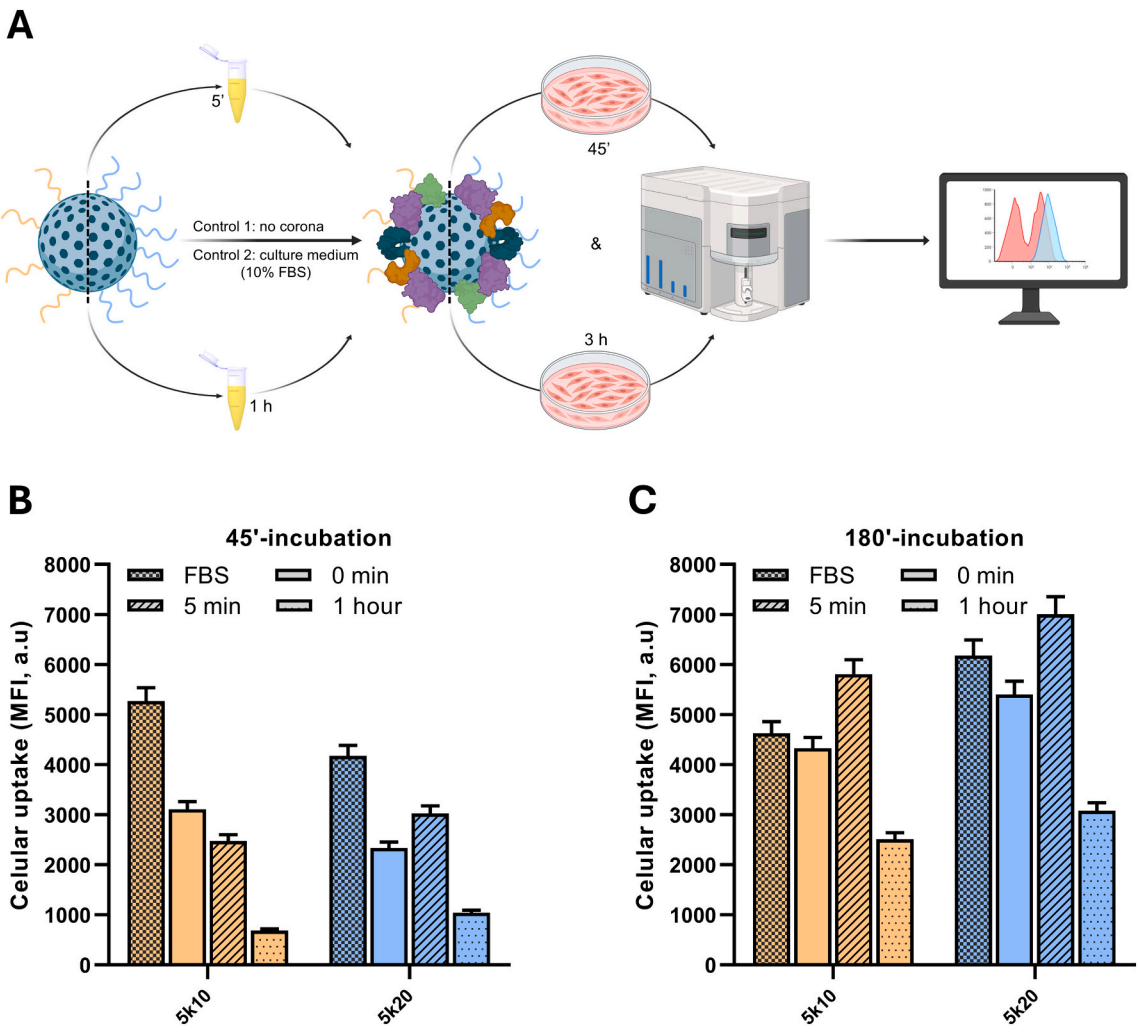

Fig. 4. Influence of protein corona on immune recognition. (A) Schematic workflow of this experiment. Four groups are included: short-term (5 min) and long-term (1 h) incubations with plasma, absence of corona (0 min), and NPs in FBS-containing culture medium (FBS). Cellular uptake was measured by flow cytometry at two time points to find out the uptake kinetics. (B) Cellular uptake after 45 min of interaction with macrophages. (C) Cellular uptake after 180 min of interaction with macrophages.

phenomenon remains unclear and warrants further research. A tentative explanation might rely on the denaturation over time of certain proteins in the corona. In this regard, it has been shown that nanoparticles are less internalized in macrophages following protein denaturation in the protein corona. In contrast, unfolded conformation led to increased immune recognition [28].

There are two generally accepted arguments in nanomedicine that are related: (i) NPs acquire a protein corona following bloodstream administration; (ii) NPs are rapidly removed from the bloodstream as they are recognized by the immune system. Hence, our initial question was: what if such observation is consequence of a transient *bad* corona that triggers early immune recognition? Thus, the rationale for choosing those time points was to recreate the initial stage after administration (5 min) and that after circulating for a longer period (1 h), *i.e.*, elucidate if such transient *bad* corona exists and modulates macrophage recognition. Regarding PEGylated NPs, experimental evidence demonstrates that they undergo accelerated bloodstream clearance (ABD) after repeated administration owing to the appearance of PEG antibodies [29]. Fig. 4 would underpin the idea that such undesired corona exists and opens the door to evaluating whether this early biological identity is linked to the ABD phenomenon.

Nonetheless, the protein corona and how it mediates interactions with cells is a complex and intricated phenomenon that is far from being well understood. In this sense, focusing on just one protein or type of protein might lead to misleading conclusions. For instance, the abundance of complement proteins increased after 1 h in both cases (Fig. 3C), which should imply higher macrophage uptake [30]. However, Fig. 4B-C demonstrate the opposite, which might be ascribed to the enrichment in APOE (Fig. 3D), since it functions as a dysopsonin that makes nanomaterials less susceptible to macrophage recognition [31]. In line with this, a positive correlation has been found between ITIH4 abundance and NP uptake in certain cell lines [32]. Hence, the drastic reduction in ITIH4 after 1 h might also support the reduced cellular uptake observed after the long-term incubation (Fig. 3E). Similarly, increased presence of HRG has been linked to reduced uptake in some cell lines [33] and macrophages [34]. Hence, the increment in HRG after 1 h of incubation (Fig. S4A) would also agree with the reduced uptake observed in both 5k-1 h. In summary, it can be concluded that it is the full array of adsorbed proteins (and how they are distributed within the protein corona [35]) what confers the NP biological identity and, consequently, what dictates how nanomedicines behave in biological systems.

4. Conclusions

In this work, we have employed PEGylated MSNs as a model platform to shed light on the following questions: (i) is the biological

identity imparted by the gold-standard, stealth polymer consistent over time? (ii) should the Vroman effect appear, would it be relevant enough to govern macrophage recognition? We have thoroughly analyzed the protein corona using short-term (5 min) and long-term (1 h) incubations with human plasma. The rationale for doing that was to find out whether an initial transient *bad* corona exists, because it could help to understand why NPs start to be removed from the bloodstream as they are injected. Our data demonstrates that the biological identity of PEGylated NPs varies over time, validating the existence of an underlying Vroman effect. Deep proteomics analyses have revealed overall protein abundance changes as a function of time, along with proteins unique to each group depending on the incubation time and PEG density. We have verified that the amount of proteins adsorbed onto the NPs surface varies in a time-dependent manner, being higher at the beginning, and leading also to differences in NP size. In addition to validating the already published observation that it is not the PEG alone, but the corona induced after 1 h what imparts stealth properties, our results suggest the existence of such transient bad corona, as demonstrated by the differential macrophage uptake of the NPs bearing the short-term protein corona.

The implications of this research go beyond the protein corona of PEGylated NPs. Yet the Vroman effect has traditionally been thought to be part of this phenomenon, we provide evidence that it could have a major role in how NPs are distributed in a living body. In this sense, even though incubating nanomaterials with proteins for 1 h is a standardized protocol to create a protein corona [36–38], our results suggest that focusing on such a comparatively long time point would overlook critical early temporal dynamics that could help to explain the clearance process. In addition to helping to understand those clearance kinetics, the assay should have implications in the screening of libraries of nanomaterials, since it would allow to discard those unable to avoid macrophage recognition regardless of the incubation time.

As discussed, the protein corona is such a complex phenomenon that it is hard to isolate the influence of individual proteins or groups of proteins from the whole array of proteins. We suggest incorporating this straightforward assay into the evaluation of any moiety claiming to impart stealth properties and, in general, into the evaluation of any nanomedicine. In this sense, there are some limitations to our proof of concept assay that should be discussed and carefully considered for implementation in different laboratory set ups. First of all, it is a bidimensional *in vitro* assay which might not exactly reflect nanomaterial-cell interactions. Nonetheless, the rationale of the assay could be transferred to 3D cellular models, thereby providing more accurate assessment of immune recognition. In addition, the amount of plasma employed in the assay could be tuned to match specific biological conditions, since plasma/nanomaterial ratio has been shown to affect the protein corona [39] and, presumably, immune recognition. Moreover, the protocol for isolating the protein corona has been shown to influence corona composition [40] and, consequently, could be further explored when implementing this approach in different laboratory set ups. Furthermore, the long-term analysis has been limited to 1 h, which might not be long enough for all nanoformulations. In spite of that, this approach should help to reduce side effects and increase biocompatibility, since researchers would be able to elucidate the optimal protein corona that leads to the lowest immune recognition and damage to immune cells. Furthermore, it could help improve NP design by discarding those nanoformulations that offer poor biological and/or physicochemical performance (*e.g.*, stability in protein-containing media), thereby facilitating scalability of the leading candidate.

In summary, this assay provides a facile approach to assess the whole contribution of a given protein corona. The results derived from this assay would be useful to avoid unnecessary animal experiments (3Rs principles) if the NPs are shown to be highly captured by the immune system following administration. Furthermore, it opens the door to bypass such transient *bad* corona by preincubating the NPs with plasma from the patient. In this manner, they would receive only NPs bearing a less *appealing* protein corona that might help to ameliorate bloodstream clearance and increase their therapeutic effect. Finally, this study has the potential to improve nanomaterial design. While our focus is on MSNs and macrophage internalization, the findings suggest that strategically modulating the protein corona would significantly enhance nanomaterial performance. Furthermore, should the therapeutic target of a nanomaterial be the immune system, finding out the protein corona that triggers the highest immune recognition would lead to increased targeting features and, consequently, increased immune modulation. Therefore, future designs of diverse nanomaterials [41–43] should account for protein corona formation to optimize their efficacy and facilitate scalability and health impact.

CRediT authorship contribution statement

Alejandro Cortés-Bazo: Software, Methodology, Investigation, Formal analysis, Data curation, Writing – review & editing. **José C. García-Perdiguero:** Validation, Software, Methodology, Investigation, Formal analysis, Data curation, Writing – review & editing. **Natividad Gómez-Cerezo:** Validation, Supervision, Software, Methodology, Investigation, Funding acquisition, Formal analysis, Data curation, Conceptualization, Writing – review & editing, Writing – original draft. **Miguel Gisbert-Garzarán:** Validation, Supervision, Software, Methodology, Investigation, Funding acquisition, Formal analysis, Data curation, Conceptualization, Writing – review & editing, Writing – original draft. **María Vallet-Regí:** Supervision, Funding acquisition, Writing – review & editing.

Funding

This study was financially supported by the following grants: (MAD2D-CM)-UCM project funded by Comunidad de Madrid, by the Recovery, Transformation and Resilience plan, and by Next Generation EU from the European Union (PR47/21-MAD2D-CM); from the European Research Council (ERC-2015-AdG, VERDI, Grant No. 694160); nanoPROT (PR17/24-31921) and MacrOArt (PR17/24-31923) projects funded by Universidad Complutense de Madrid and Comunidad de Madrid (Convenio para la concesión de una subvención directa para el fomento y promoción de la investigación y la transferencia de tecnología durante el periodo 2023–2026).

Declaration of competing interest

The authors declare that they have no known competing financial interests or personal relationships that could have appeared to influence the work reported in this paper.

Acknowledgments

This study was financially supported by the following grants: (MAD2D-CM)-UCM project funded by Comunidad de Madrid, by the Recovery, Transformation and Resilience plan, and by Next Generation EU from the European Union (PR47/21-MAD2D-CM); from the European Research Council (ERC-2015-AdG, VERDI, Grant No. 694160); nanoPROT (PR17/24-31921) and MacrOArt (PR17/24-31923) projects funded by Universidad Complutense de Madrid and Comunidad de Madrid (Convenio para la concesión de una subvención directa para el fomento y promoción de la investigación y la transferencia de tecnología durante el periodo 2023-2026). A.C-B and J.C.G-P acknowledge the Fundación Ramón Areces for their PhD fellowships. We would also like to thank the Centro Nacional de Microscopía Electrónica (Universidad Complutense de Madrid, Spain) and the Proteomics facility of the National Center for Biotechnology (Spain) for their technical assistance.

Appendix A. Supplementary data

The Supporting Information includes (i) an excel file with all proteins

detected; (ii) a text file with physicochemical characterization (FTIR spectroscopy), proteomics (numerical values and top 100 & top 20 analyses), and cellular experiments (cell viability, additional flow cytometry data). Supplementary data to this article can be found online at [https://doi.org/10.1016/j.ijbiomac.2026.152050].

Data availability

Data will be made available on request.

References

[1] M.P. Monopoli, C. Åberg, A. Salvati, K.A. Dawson, Biomolecular coronas provide the biological identity of nanosized materials, Nat. Nanotechnol. 7 (2012) 779–786.
[2] T. Kopac, Protein corona, understanding the nanoparticle–protein interactions and future perspectives: a critical review, Int. J. Biol. Macromol. 169 (2021) 290–301.
[3] R. Bilardo, F. Traldi, A. Vdovchenko, M. Resmini, Influence of surface chemistry and morphology of nanoparticles on protein corona formation, WIREs Nanomedicine and Nanobiotechnology 14 (2022) e1788.
[4] E. Blanco, H. Shen, M. Ferrari, Principles of nanoparticle design for overcoming biological barriers to drug delivery, Nat. Biotechnol. 33 (2015) 941–951.
[5] G. Berrecoso, J. Crecente-Campo, M.J. Alonso, Unveiling the pitfalls of the protein corona of polymeric drug nanocarriers, Drug Deliv. Transl. Res. 10 (2020) 730–750.
[6] Y. Duan, R. Coreas, Y. Liu, D. Bitounis, Z. Zhang, D. Parviz, M. Strano, P. Demokritou, W. Zhong, Prediction of protein corona on nanomaterials by machine learning using novel descriptors, NanoImpact 17 (2020) 100207.
[7] T. Kopac, Leveraging Artificial Intelligence and Machine Learning for Characterizing Protein Corona, Nanobiological Interactions, and Advancing Drug Discovery, Bioengineering 12 (2025).
[8] B.P. Stordy, Z. Sepahi, G.D. Patrón, W. Yang, A.D. Goodson, C. Blackadar, A. J. Tavares, G. Lin, A. Malekjahani, B. Ling, R. Ravichandran, D.R. Hicks, M. G. Shapiro, M. Zhang, N.P. King, D. Baker, L.A. Ricardez-Sandoval, W.C.W. Chan, The binding affinities of serum proteins to nanoparticles, J. Am. Chem. Soc. 147 (2025) 20475–20492.
[9] M. Li, S. Jiang, J. Simon, D. Paßlick, M.-L. Frey, M. Wagner, V. Mailänder, D. Crespy, K. Landfester, Brush conformation of polyethylene glycol determines the stealth effect of nanocarriers in the low protein adsorption regime, Nano Lett. 21 (2021) 1591–1598.
[10] N. Bertrand, P. Grenier, M. Mahmoudi, E.M. Lima, E.A. Appel, F. Dormont, J.-M. Lim, R. Karnik, R. Langer, O.C. Farokhzad, Mechanistic understanding of in vivo protein corona formation on polymeric nanoparticles and impact on pharmacokinetics, Nat. Commun. 8 (2017) 777.
[11] Z.W. Richter-Bisson, H.-Y. Nie, K. Nygard, Y.S. Hedberg, Protein displacement dynamics on chromium oxide nanoparticles: Investigating the Vroman effect in a binary protein system, Colloids Surf. A Physicochem. Eng. Asp. 719 (2025) 136985.
[12] O. Vilanova, J.J. Mittag, P.M. Kelly, S. Milani, K.A. Dawson, J.O. Rädler, G. Franzese, Understanding the kinetics of protein–nanoparticle corona formation, ACS Nano 10 (2016) 10842–10850.
[13] S. Ferdosi, A. Stukalov, M. Hasan, B. Tangeysh, T.R. Brown, T. Wang, E. M. Elgierari, X. Zhao, Y. Huang, A. Alavi, B. Lee-McMullen, J. Chu, M. Figa, W. Tao, J. Wang, M. Goldberg, E.S. O'Brien, H. Xia, C. Stolarczyk, R. Weissleder, V. Farias, S. Batzoglou, A. Siddiqui, O.C. Farokhzad, D. Hornburg, Enhanced competition at the nano–bio interface enables comprehensive characterization of protein corona dynamics and deep coverage of proteomes, Adv. Mater. 34 (2022) 2206008.
[14] H. Yang, S. Lu, S. Wang, L. Liu, B. Zhu, S. Yu, S. Yang, J. Chang, Evolution of the protein corona affects macrophage polarization, Int. J. Biol. Macromol. 191 (2021) 192–200.
[15] C. Pisani, J.-C. Gaillard, M. Odorico, J.L. Nyalosaso, C. Charnay, Y. Guari, J. Chopineau, J.-M. Devoisselle, J. Armengaud, O. Prat, The timeline of corona formation around silica nanocarriers highlights the role of the protein interactome, Nanoscale 9 (2017) 1840–1851.
[16] S. Tenzer, D. Docter, J. Kuharev, A. Musyanovych, V. Fetz, R. Hecht, F. Schlenk, D. Fischer, K. Kiouptsi, C. Reinhardt, K. Landfester, H. Schild, M. Maskos, S. K. Knauer, R.H. Stauber, Rapid formation of plasma protein corona critically affects nanoparticle pathophysiology, Nat. Nanotechnol. 8 (2013) 772–781.
[17] A.L. Barrán-Berdón, D. Pozzi, G. Caracciolo, A.L. Capriotti, G. Caruso, C. Cavaliere, A. Riccioli, S. Palchetti, A. Laganà, Time evolution of nanoparticle–protein corona in human plasma: relevance for targeted drug delivery, Langmuir 29 (2013) 6485–6494.
[18] N.P. Mortensen, G.B. Hurst, W. Wang, C.M. Foster, P.D. Nallathamby, S.T. Retterer, Dynamic development of the protein corona on silica nanoparticles: composition and role in toxicity, Nanoscale 5 (2013) 6372–6380.
[19] M. Manzano, M. Vallet-Regí, Mesoporous silica nanoparticles for drug delivery, Adv. Funct. Mater. 30 (2020) 1902634.
[20] T.M. Göppert, R.H. Müller, Adsorption kinetics of plasma proteins on solid lipid nanoparticles for drug targeting, Int. J. Pharm. 302 (2005) 172–186.
[21] J.J. Aguilera-Correa, Y. Tasrini, M. Gisbert-Garzarán, A. Boulay, T. Carvalho, F. P. Blanchet, M. Vallet-Regí, L. Kremer, In vivo antimicrobial activity of engineered mesoporous silica nanoparticles targeting intracellular mycobacteria, Nat. Commun. 16 (2025) 7388.
[22] J.C. García-Perdiguero, N. Gómez-Cerezo, M. Gisbert-Garzarán, M. Manzano, M. Vallet-Regí, Unraveling the role of calcium in the osteogenic behavior of mesoporous bioactive glass nanoparticles, Acta Biomater. 198 (2025) 482–496.
[23] F. Millozzi, P. Milán-Rois, A. Sett, G. Delli Carpini, M. De Bardi, M. Gisbert-Garzarán, M. Sandonà, C. Rodríguez-Díaz, M. Martínez-Mingo, I. Pardo, F. Esposito, M.T. Viscomi, M. Bouché, O. Parolini, V. Saccone, J.-J. Toulmé, Á. Somoza, D. Palacios, Aptamer-conjugated gold nanoparticles enable oligonucleotide delivery into muscle stem cells to promote regeneration of dystrophic muscles, Nat. Commun. 16 (2025) 577.
[24] D. Nevozhay, R. Rauch, Z. Wang, K.V. Sokolov, Optimal size and PEG coating of gold nanoparticles for prolonged blood circulation: a statistical analysis of published data, Nanoscale Adv. 7 (2025) 722–727.
[25] S. Hak, E. Helgesen, H.H. Hektoen, E.M. Huuse, P.A. Jarzyna, W.J.M. Mulder, O. Haraldseth, C.L. de Davies, The effect of nanoparticle polyethylene glycol surface density on ligand-directed tumor targeting studied in vivo by dual modality imaging, ACS Nano 6 (2012) 5648–5658.
[26] K. Yang, C. Reker-Smit, M.C.A. Stuart, A. Salvati, Effects of protein source on liposome uptake by cells: corona composition and impact of the excess free proteins, Adv. Healthc. Mater. 10 (2021) 2100370.
[27] S. Schöttler, G. Becker, S. Winzen, T. Steinbach, K. Mohr, K. Landfester, V. Mailänder, F.R. Wurm, Protein adsorption is required for stealth effect of poly (ethylene glycol)- and poly(phosphoester)-coated nanocarriers, Nat. Nanotechnol. 11 (2016) 372–377.
[28] Y. Yan, K.T. Gause, M.M.J. Kamphuis, C.-S. Ang, N.M. O'Brien-Simpson, J. C. Lenzo, E.C. Reynolds, E.C. Nice, F. Caruso, Differential roles of the protein corona in the cellular uptake of nanoporous polymer particles by monocyte and macrophage cell lines, ACS Nano 7 (2013) 10960–10970.
[29] J. Pan, Y. Wang, Y. Chen, C. Zhang, H. Deng, J. Lu, W. Chen, Emerging strategies against accelerated blood clearance phenomenon of nanocarrier drug delivery systems, J. Nanobiotechnol. 23 (2025) 138.
[30] J.R. Dunkelberger, W.-C. Song, Complement and its role in innate and adaptive immune responses, Cell Res. 20 (2010) 34–50.
[31] X. Lu, P. Xu, H.-M. Ding, Y.-S. Yu, D. Huo, Y.-Q. Ma, Tailoring the component of protein corona via simple chemistry, Nat. Commun. 10 (2019) 4520.
[32] S. Ritz, S. Schöttler, N. Kotman, G. Baier, A. Musyanovych, J. Kuharev, K. Landfester, H. Schild, O. Jahn, S. Tenzer, V. Mailänder, Protein corona of nanoparticles: distinct proteins regulate the cellular uptake, Biomacromolecules 16 (2015) 1311–1321.
[33] A. Aliyandi, C. Reker-Smit, R. Bron, I.S. Zuhorn, A. Salvati, Correlating corona composition and cell uptake to identify proteins affecting nanoparticle entry into endothelial cells, ACS Biomater. Sci. Eng. 7 (2021) 5573–5584.
[34] C. Fedeli, D. Segat, R. Tavano, L. Bubacco, G. De Franceschi, P.P. de Laureto, E. Lubian, F. Selvestrel, F. Mancin, E. Papini, The functional dissection of the plasma corona of SiO2-NPs spots histidine rich glycoprotein as a major player able to hamper nanoparticle capture by macrophages, Nanoscale 7 (2015) 17710–17728.
[35] Y. Qiu, T. He, C. Miao, X. Shi, Y. Niu, V. Mailänder, D. Crespy, K. Landfester, S. Jiang, The distribution of complement proteins in soft and hard coronas impacts macrophage uptake of nanoparticles, Adv. Healthc. Mater. 15 (2026) e03534.
[36] L.E. González-García, M.N. Macgregor, R.M. Visalakshan, A. Lazarian, A. A. Cavallaro, S. Morsbach, A. Mierczynska-Vasilev, V. Mailänder, K. Landfester, K. Vasilev, Nanoparticles surface chemistry influence on protein corona composition and inflammatory responses, Nanomaterials 12 (2022).
[37] V. Castagnola, V. Tomati, L. Boselli, C. Braccia, S. Decherchi, P.P. Pompa, N. Pedemonte, F. Benfenati, A. Armirotti, Sources of biases in the in vitro testing of nanomaterials: the role of the biomolecular corona, Nanoscale Horiz. 9 (2024) 799–816.
[38] M.D. Ghouri, A. Tariq, J. Saleem, A. Muhaymin, R. Cai, C. Chen, Protein corona potentiates the recovery of nanoparticle-induced disrupted tight junctions in endothelial cells, Nanoscale Horiz. 10 (2025) 179–189.
[39] M.P. Monopoli, D. Walczyk, A. Campbell, G. Elia, I. Lynch, F. Baldelli Bombelli, K. A. Dawson, Physical−chemical aspects of protein corona: relevance to in vitro and in vivo biological impacts of nanoparticles, J. Am. Chem. Soc. 133 (2011) 2525–2534.
[40] L. Böhmert, L. Voß, V. Stock, A. Braeuning, A. Lampen, H. Sieg, Isolation methods for particle protein corona complexes from protein-rich matrices, Nanoscale Adv. 2 (2020) 563–582.
[41] N. Andrikopoulos, H. Tang, Y. Wang, X. Liang, Y. Li, T.P. Davis, P.C. Ke, Exploring peptido-nanocomposites in the context of amyloid diseases, Angew. Chem. Int. Ed. 63 (2024) e202309958.
[42] J. Ren, N. Andrikopoulos, K. Velonia, H. Tang, R. Cai, F. Ding, P.C. Ke, C. Chen, Chemical and biophysical signatures of the protein corona in nanomedicine, J. Am. Chem. Soc. 144 (2022) 9184–9205.
[43] V. Palmieri, G. Caracciolo, Tuning the immune system by nanoparticle–biomolecular corona, Nanoscale Adv. 4 (2022) 3300–3308.